VOLUME 8 (SPECIAL ISSUE) 2022

ISSN 2454-3055

Manuscripts under Special issue are published with the Theme "Modern Perspectives of Biological Sciences"

Guest Editor: Dr. S. Mohanasundaram
Assistant Guest Editor: Dr. S.S. Syed Abuthahir

INTERNATIONAL JOURNAL OF ZOOLOGICAL INVESTIGATIONS

Forum for Biological and Environmental Sciences

Published by Saran Publications, India

International Journal of Zoological Investigations Vol. 8, Special Issue, 1-6 (2022)

International Journal of Zoological Investigations

Contents available at Journals Home Page: www.ijzi.net

Editor-in-Chief: Prof. Ajai Kumar Srivastav

Published by: Saran Publications, Gorakhpur, India

ISSN: 2454-3055

TiO_2@ZnO–CdS Nanocomposites for Sensing and Cytotoxicity Applications

Usha Rani C.[1], Pragathiswaran C.[1*], Balakrishnan D.[1], Selvarani K.[1] and Smitha C.[2]

[1]Post –Graduate and Research Department of Chemistry, Periyar EVR College (Affiliated to Bharathidasan University, Trichy 24), Trichy 620023, India

[2]Government College of Engineering, Trichy 620012, India

**Corresponding Author*

Received: 4th August, 2022; **Accepted:** 22nd August, 2022; **Published online:** 15th September, 2022

https://doi.org/10.33745/ijzi.2022.v08i0s.001

Abstract: In this study the sol-gel method was used to create a composite of titanium oxide nanoparticles (TiO_2-NPs) @ ZnO nanoparticles (TiO_2 @ ZnO). Using a hydrothermal process, the TiO_2@ZnO nanocomposite (NC) was changed via wreathing cadmium sulphide nanoparticles (CdS NPs) (TiO_2@ZnO–CdS). Fourier transform infrared spectroscopy (FTIR), scanning electron microscopy (SEM), and energy-dispersive X-ray spectroscopy (EDAX) were employed to investigate the TiO_2@ZnO–CdS NC. The CdS NPs are uniformly distributed over the TiO_2@ZnO NC. According to FESEM analysis. TiO_2@ZnO–CdS NC is used to detect imidazole at low concentrations and assess cytotoxicity. The TiO_2@ZnO–CdS NC has been found to have the best electrochemical sensing activity and considerable cytotoxicity against A549 lung cancer cells.

Keywords: Nanocomposite, Sol-gel method, Sensing activity, Cytotoxicity, Lung cancer cells

Citation: Usha Rani C., Pragathiswaran C., Balakrishnan D., Selvarani K. and Smitha C.: TiO_2@ZnO–CdS nanocomposites for sensing and cytotoxicity applications. Intern. J. Zool. Invest. 8(Special Issue): 1-6, 2022.
https://doi.org/10.33745/ijzi.2022.v08i0s.001

Introduction

The photocatalytic approach has gained popularity among the approaches used to degrade environmental contaminants. Titanium dioxide nanoparticles (TiO_2 NPs) have a significant oxidising power, which makes them suitable for solar cells, supercapacitors, sensors, water treatment, and photocatalytic dye deterioration when exposed to light. The TiO_2 is accessible in different composite forms, including TiO_2@Fe_2O_3, GO@TiO_2, TiO_2@ZnO@Ag and MoS_2@TiO_2. This nanocomposite (NC) significantly improves the semiconductor-based photocatalytic demand for capturing incident light, and new energy generates electron-hole transforms to reduce electron-hole and quick recombination. The goal of this study was to modify TiO_2 NPs that have been engineered using ZnO NPs and then adorned with CdS NPs using a hydrothermal technique. The sensing and cytotoxicity activity of TiO_2/ZnO–CdS nanocomposites (NCs) was investigated further after their manufacture (Luo *et al*., 2015; Pragathiswaran *et al*., 2015, 2022; Cruz *et al*., 2017).

Materials and Methods

Titanium (IV) chloride ($TiCl_4$), Cetyltrimethyl ammonium bromide (CTAB), tetraethyl orthosilicate (TEOS), cadmium nitrate (Cd $NO_3.4H_2O$), sodium sulphide ($Na_2S.9H_2O$), 100% methanol, ethanol, and ammonium hydroxide (NH_4OH) were of Analar reagents.

Synthesis of TiO_2-NPs:

$TiCl_4$ (9 ml) was progressively added to deionized water with ice bath while steadily stirring till fully dissolved, then 18 ml of 30% NH_4OH was added to resultant solution. One hour was given for the resultant titanium hydroxide ($Ti(OH)_4$) to stand. TiO_2 NPs were filtered, washed with deionized water (DW), and dried in a vacuum oven at 100 °C for three hours.

Fabrication of TiO_2@ZnO–CdS NC:

TiO_2 (1 g) and 1M $ZnSO_4$ (60 ml) were infused dropwise into 2M NH_4CO_3 (30 ml) solution while aggressively agitating at 600 °C for 1 h. The resultant was filtered and rinsed three times with double-distilled water and ethanol before being dried in a vacuum oven at 60 °C for 24 h. The resultant was calcined for 1 h at 600 °C to yield TiO_2/ZnO powder. CdS NPs were dropped onto the surface of the TiO_2@ZnO NC by chemical reduction method. TiO_2@ZnO NC (1g) was disseminated in DW (250 ml) with constant agitating for 30 min. 0.4 mmol L^{-1} of $Cd(NO_3).24\ H_2O$, and 1.5 mmol L^{-1} of Na_2S was added. Twenty milliliters of water and pure ethanol were mixed with 0.03 mmol L^{-1} glutathione. 1 g of TiO_2/ZnO NC was wrapped in an autoclave, and incubated at 453 K for three and half hours. The TiO_2/ZnO–CdS NC was formed after the reaction by rinsing the ensuing sample with deionized water and pure ethanol and drying it overnight.

Characterization:

FESEM and EDAX were used to examine the morphology, and elemental analysis of TiO_2@ZnO–CdS NC, respectively. FTIR (Shimadzu-650) spectroscopy was used to examine the functional groups of the NC.

Electrochemical characteristics on the electrode surface:

The glassy carbon electrode (GCE) is incorporated in the presence and absence of imidazole to determine oxidation and reduction of CV peak current. Figure 1 shows the CV peak currents of bare GCE. The peak current of oxidation was determined to be 0.2 x10 $^{-4}$A without Imidazole and 0.2×10^{-4} A with imidazole. The reduction peak current was found to be 1.0×10^{-4} A without imidazole and 2.6×10^{-4} A. with imidazole.

Cytotoxicity measurement:

DCFH-DA reactive oxygen species (ROS) detection kit (S0033) was obtained from Abcam. The A549 lung cancer cells were seeded at the concentration of 10^4 cells at 96 well plates and allowed to attach for 5 h. Then the TiO_2@ZnO–CdS dissolved RPMI medium was exposed to the cells at 40 and 120 μg/ml for 6 h. After that, the cells were rinsed in PBS and stained with DCFH-DA for 45 min. The cells were then rinsed in wash buffers and examined using fluorescence microscopy.

Results and Discussion

Surface morphology investigation:

FESEM pictures show that all investigative NCs have a homogeneous structure and spherical shape (Figs. 1a-c). The CdS NPs are equally distributed across the spherical surface of the TiO_2@ZnO NC. The post-annealing process could make the porous nature of the TiO_2@ZnO–CdS [Lee *et al*., 2015; Yu *et al*., 2015; Harinee *et al*., 2022]. The results of TiO_2@ZnO–CdS NC elemental analysis for EDAX spectrum demonstrated the existence of Ti, Si, O, Cd and S in hybrid material formation as shown in Figure 1d.

Analysis of FTIR:

As shown in Figure 2, the FTIR spectra of TiO_2 NP, TiO_2@ZnO, and TiO_2@ZnO–CdS NC were carried out and recorded. The peaks at 456 and 532 cm^{-1} were ascribed with Ti–O–Ti stretching vibration. The bands about 3750 and 1700 cm^{-1} for bending

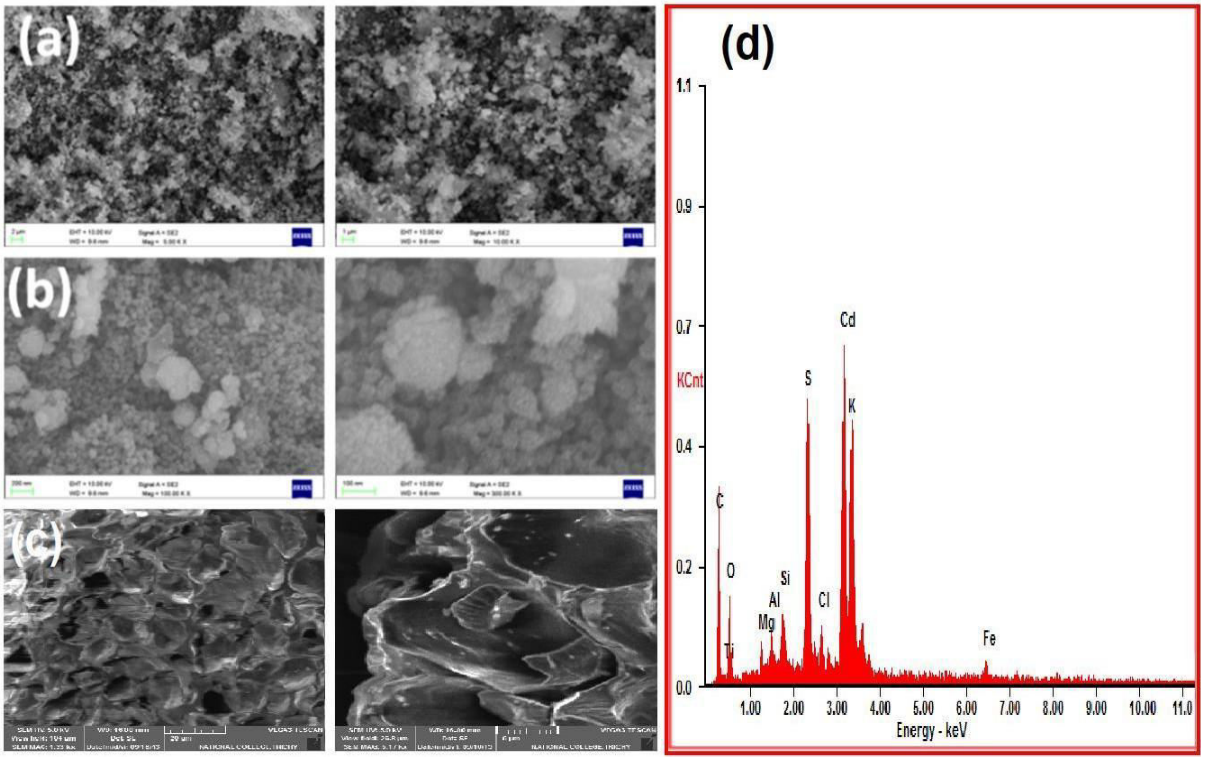

Fig.1: FESEM image of (a) TiO2 NPs (b) TiO2@ZnO (c) TiO2@ZnO–CdS (d) EDAX- spectrum.

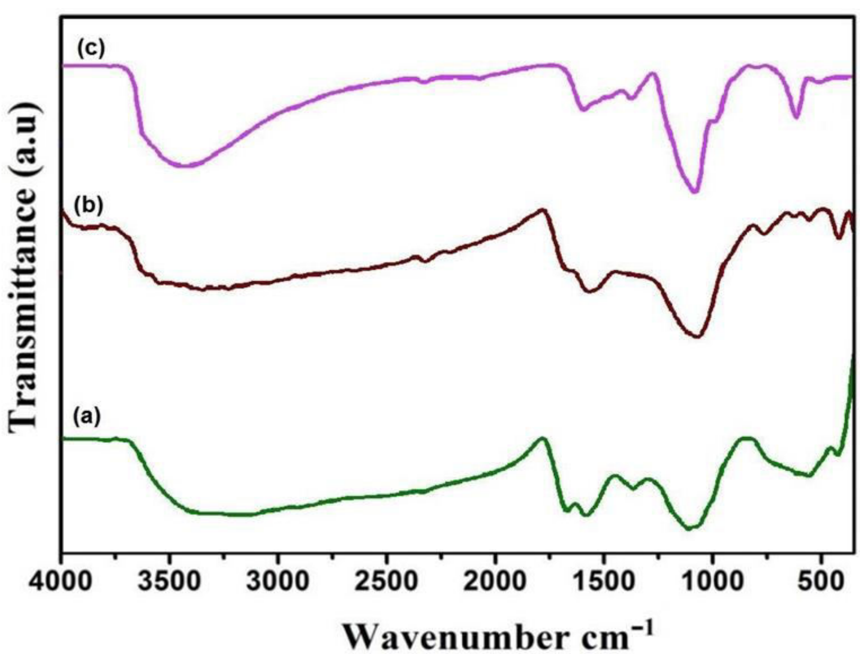

Fig. 2: FTIR spectra of (a) TiO2 NP (b) TiO2@ZnO (c) TiO2 @ ZnO–CdS NC.

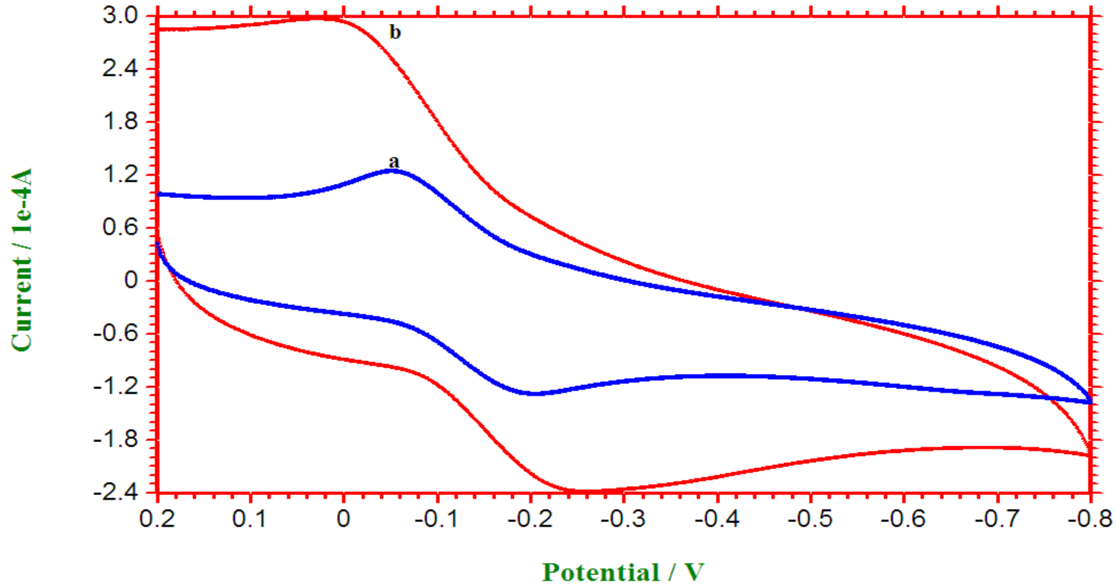

Fig. 3: Cyclic Voltammetry of (a) GCE without imidazole and (b) GCE with imidazole in HCl containing 1.0×10-4 M.

and stretching vibrations of –OH and adsorbed H_2O, respectively. Peaks generated at wave numbers of 1360 and 1250 cm^{-1} in TiO_2@ZnO–CdS NC might be attributed to the symmetric and asymmetric stretching waves of Zn – O – Zn in ZnO in the NC. Ti–O–Zn waves were detected at 621 and 786 cm^{-1}.

Electrochemical determination of imidazole:

The CV technique is a popular and successful approach for investigating properties of modified GCE electrodes: (a) TiO2, (b) TiO2 @ ZnO/GCE, (c) TiO2 @ ZnO–CdS/GCE and (d) TiO2 @ ZnO–CdS/GCE with 1.0 x 10-4 M Imidazole. Figure 1 shows the modified electrodes with and without imidazole, as well as the CV peak currents of bare GCE (Figs. 3, 4). Without imidazole, the oxidation peak current was determined to be 0.3 $X10^{-4}$ (a) and 0.3 X 10^{-4} A with imidazole. The anodic current increased due to the addition of NPs. The cathodic peak current was found to be 1.0×10^{-4} (a) without imidazole and 2.9×10^{-4}A with imidazole. It indicated the larger active area of the NC, which also reflected its electron transfer property. The peak current ratio Ipa/Ipc was around 1 A. The anodic potential was observed to be -100 (a) without imidazole and -300 mV with imidazole (d). The cathodic peak potential was found to be –50 without imidazole (a) and 50 mV with imidazole (d). The difference between anodic and cathodic potential variation (ΔE) was between 100 mV and 300 mV. The anodic and cathodic peak currents continued to increase as the scan rate increased from (10–400 mVs^{-1}) while the potential practically remained constant.

Cytotoxicity assessment of TiO_2@ZnO–CdS NCs:

ROS generation played a significant role in cellular toxicity of metal and metal oxide NCs. Production of O_2^-, H_2O_2, ·OH was determined in NPs treated in cells after 24 h. TiO_2@ZnO–CdS NCs exposure increased ROS production and disrupted redox equilibrium. Cellular ROS levels of A549 lung cancer cells treated with 40 μg ml^{-1} expressed the significant percentage of ROS while the increasing level of ROS was observed at the higher dosage (120 μg ml^{-1}) of NC treatment (Fig. 5). Fluorescence microscopy images representing the green fluorescence of DCF uptake (ROS generation) in A549 cells were corroborated with the oxidative stress-related toxicity of synthesized NCs (Popescu *et al*., 2015; Shao *et al*., 2015; Cao *et al*., 2015). The excessive ROS generation on the cellular environment induced the metabolic changes which affected the protein regulation pathways and destroys the cancerous cells. The resultant data confirmed the

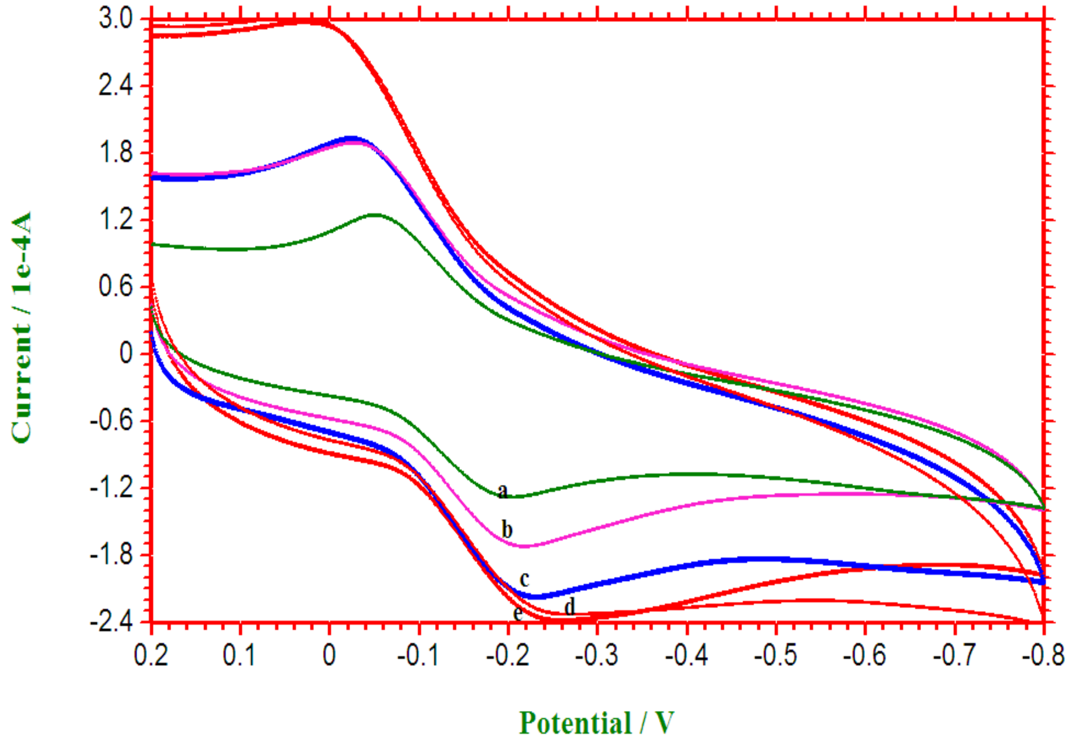

Fig. 4; CV response of bare GCE (a) TiO2@ ZnO/GCE, (b) TiO2 @ZnO–CdS/GCE, (c) TiO2@ZnO–CdS/GCE with 1.0×10-4 M imidazole.

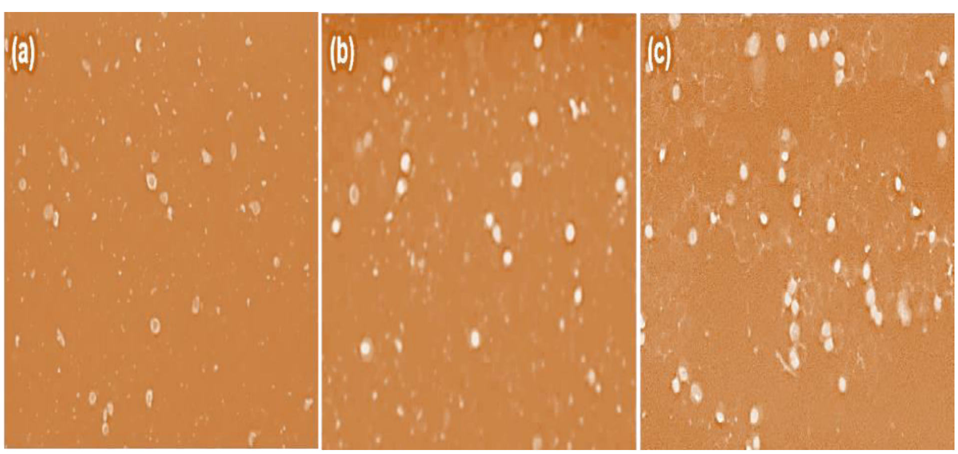

Fig. 5: Fluorescence microscopy analysis of intracellular ROS level Untreated control cells (a), 40 and 120 μg ml^{-1} TiO2@ZnO–CdS exposed cells (b) and (c) respectively.

acceleration of ROS generation was driven by the combined effect of TiO_2@ZnO–CdS NCs in a dose-dependent manner (Ma *et al*., 2015; Mary *et al*., 2021; Praathiswaran *et al*., 2021).

Conclusion

Cadmium sulphide nanoparticles were wrapped around the TiO_2@ZnO NC. FESEM, EDAX, and XRD were used to characteriSe the TiO_2@ZnO–CdS NC. The TiO_2@ZnO–CdS NC showed best electrochemical sensing activity of imidazole at lower concentration and the cytotoxicity study revealed that TiO_2@ZnO–CdS had significant cytotoxicity towards A549 lung cancer cells. This is confirmed that the TiO_2@ZnO–Cd NC could be used as a photocatalysis, electrochemical sensor and anticancer material in future.

References

Cai J, Wu X, Li S, Zheng F, Zhu L and Lai Z. (2015) Synergistic effect of double-shelled and sandwiched TiO2@Au@C hollow spheres with enhanced visible-light-driven photocatalytic activity. ACS Appl. Mater Interfaces 7(6): 3764-3772.

Cruz M, Gomeza C, Duran-Valle CJ, Pastrana-Martínez LM, Faria JL, Silva MT, Faraldos M and Bahamonde A. (2017) Bare TiO_2 and graphene oxide TiO_2photocatalysts on the degradation of selected pesticides and influence of the water matrix. Appl Surf Sci. 416: 1013-1021.

Govindhan P and Pragathiswaran C. (2016 a) Synthesis and characterization of TiO_2@SiO_2–Ag nanocomposites towards photocatalytic degradation of rhodamine B and methylene blue. J Mater Sci Mater Electron, 27(8): 8778-8785.

Govindhan P and Pragathiswaran C. (2016 b) Antibacterial activity and anticancer activity of Ag doped TiO_2@SiO_2 nanocomposite. J Nanosci Technol. 2: 173-175.

Harinee S, Muthukumar K, James RA, Arulmozhic M, Dahms HU and Ashok M. (2022) Bio-approach ZnO/Ag nano-flowers: enhanced photocatalytic and photoexcited anti-microbial activities towards pathogenic bacteria. Materials Today Sustainability 18: 100133.

Karimi L, Yazdanshenas ME, Khajavi R, Rashidi A and Mirjalili M. (2016) Functional finishing of cotton fabrics using graphene oxide nanosheets decorated with titanium dioxide nanoparticles. J Text Inst. 107(9): 1122-1134.

Lee KM, Hamid SBA and Lai CW. (2015) Mechanism and kinetics study for photocatalytic oxidation degradation: A case study for phenoxyacetic acid organic pollutant, J Nanomater. 2015: 940857.

Luo B, Xu D, Li D, Wu G, Wu M, Shi W and Chen M. (2015) Fabrication of a Ag/Bi3TaO_7 plasmonic photocatalyst with enhanced photocatalytic activity for degradation of tetracycline. ACS Appl Mater Interfaces 7(31): 17061-17069.

Ma S, Zhan S, Jia Y and Zhou Q. (2015) Superior antibacterial activity of Fe3O4-TiO_2 nanosheets under solar light. ACS Appl Mater Interfaces 7(39): 21875-21883.

Mary JV, Pragathiswaran C and Anusuya N. (2021) Photocatalytic, degradation, sensing of Pb^{2+} using titanium nanoparticles synthesized via plant extract of *Cissus quadrangularis*: In-vitro analysis of microbial and anti-cancer activities. J Mol Struct. 1236: 130144.

Popescu T, Lupu AR, Raditoiu V, Purcar V and Teodorescu VS. (2015) On the photocatalytic reduction of MTT tetrazolium salt on the surface of TiO2 nanoparticles: Formazan production kinetics and mechanism. J Colloid Interface Sci. 457:108–120.

Pragathiswaran C, Smitha C, Abbubakkar BM, Govindhan P and Krishnan NA. (2015) Materials Today: Proceedings synthesis and characterization of TiO_2/ZnO – Ag nanocomposite for photocatalytic degradation of dyes and anti-microbial activity. Mater Today Proc. 45(8): 3357-3364.

Pragathiswaran C, Thulasi G, Al-ansari MM, Al-humaid LA and Saravanan M. (2021) Experimental investigation and electrochemical characterization of titanium coated nanocomposite materials for biomedical applications. J Mol Struct. 1231: 129932.

Shao W, Liu X, Min H, Dong G, Feng D and Zuo S. (2015) Preparation, characterization, and antibacterial activity of silver nanoparticle-decorated graphene oxide nanocomposite. ACS Appl Mater Interfaces 7(12): 6966-6973.

Yu Y, He T, Guo L, Yang Y, Guo L, Tang Y and Cao Y. (2015) Efficient visible-light photocatalytic degradation system assisted by conventional Pd catalysis. Sci Rep. 5: 1-6.